*Traffic 2002; **3**: 110–123*
Munksgaard International Publishers

ISSN 1398-9219

Ubiquitin-Independent Entry into the Yeast Recycling Pathway

Linyi Chen[1] and Nicholas G. Davis[2,*]

[1] Department of Physiology, University of Michigan School of Medicine, Ann Arbor, MI 48109, USA
[2] Departments of Surgery and Pharmacology, Wayne State University School of Medicine, Detroit, MI 48201, USA
** Corresponding author: Nicholas G. Davis, ndavis@cmb.biosci.wayne.edu*

The yeast a-factor receptor (Ste3p) is subject to two mechanistically distinct modes of endocytosis: a constitutive, ligand-independent pathway links to vacuolar degradation of the receptor, while a ligand-dependent uptake pathway links primarily to recycling and thus, receptor reutilization. Ste3p ubiquitination triggers its uptake into the constitutive pathway. The present work considers the role of the receptor ubiquitination associated with the Ste3p ligand-dependent endocytosis mechanism. The *doa4Δ* mutation which reduces the cellular availability of ubiquitin blocks the Ste3p constitutive uptake. Uptake into the Ste3p ligand-dependent recycling pathway, however, continues unimpaired. The ubiquitin independence of Ste3p ligand-dependent uptake was further indicated by analysis of receptor mutants having Lys-to-Arg substitutions at all possible ubiquitin acceptor sites. Again, the ligand-induced internalization was unimpaired. Furthermore, no discernible effect was seen on either recycling or on the slow *PEP4*-dependent turnover of the receptor (for receptor internalized via the ligand-dependent mechanism, trafficking to the vacuole/lysosome is the minor, alternate fate to recycling). However, one striking effect of the Lys-to-Arg mutations was noted. Following a prolonged exposure of the cells to the a-factor ligand, rather than being delivered to the vacuolar lumen, the Lys-to-Arg receptor was found to localize instead to the limiting membrane of the vacuole. Thus, while receptor ubiquitination clearly is not required for either the a-factor-dependent uptake into recycling pathway or for the recycling itself, it does affect the routing of receptor to the vacuole, likely by affecting the routing through the late endosomal, multivesicular body: ubiquitinated receptor may be selected into the internal, lumenal vesicles, while unmodified receptor may be left to reside at the limiting external membrane.

Key words: endocytosis, lysosome, MVB, pheromones, recycling, ubiquitin, vacuole, yeast

Received 27 September 2001, revised and accepted for publication 2 November 2001

In the yeast *Saccharomyces cerevisiae*, ubiquitin plays a central role in endocytosis. The yeast plasma membrane proteins studied to date utilize a ubiquitin-dependent endocytic mechanism. Mutational disruption of the cellular ubiquitination process blocks the cell surface internalization step and also, the subsequent degradation of internalized proteins by the yeast vacuole/lysosome (1–3). For the two yeast pheromone receptors, i.e. the **a**- and the α-factor receptors, where the role of ubiquitination in endocytosis has been well studied, attachment of a single ubiquitin moiety to the cytosolic domain of the surface-localized receptor suffices as the signal for triggering uptake (4–6). For other yeast plasma membrane proteins, short multiubiquitin chains linked through ubiquitin residue Lys-63 may be required (7,8). While prominent in yeast, a role for ubiquitin in endocytosis is not limited to the yeast cell – ubiquitin also participates in the endocytic trafficking of a variety of mammalian plasma membrane proteins (1).

The yeast **a**- and α-factor pheromone receptors (Ste3p and Ste2p, respectively) are classic G protein-coupled receptors that enable the intracellular communication which precedes the mating of haploid **a** and α cell types to the **a**/α diploid cell. Both receptors have been exploited as model systems in the study of endocytosis in yeast. For Ste3p, two distinct endocytic mechanisms which rely on different receptor signals and, to some extent, on different *trans*-acting factors are employed – a constitutive (ligand-independent) uptake mechanism and a ligand-dependent uptake mode. Ste3p constitutive endocytosis is an example of typical ubiquitin-dependent endocytosis (9). The signal directing this ligand-independent uptake is an extended, 58-residue-long PEST-like ubiquitination signal which maps to the C-terminal end of the Ste3p regulatory, cytoplasmically disposed, C-terminal domain (CTD) (Figure 1) (10). This sequence is rich in both the acidic residues aspartate and glutamate and in the hydroxylated residues serine and threonine and has three lysine residues which function redundantly as the acceptor sites for ubiquitin attachment (5). Ste3p ubiquitination requires the prior action of the redundant type I casein kinases, Yck1p and Yck2p, which apparently activate the PEST-like sequence for ubiquitination through Ser/Thr phosphorylation. Also required is the ankyrin-repeat protein Akr1p, which functions to properly localize Yck1p/Yck2p to the plasma membrane (11). Like other examples of ubiquitin-dependent uptake in yeast, Ste3p ubiquitination involves the redundant E2 ubiquitin-conjugating activities Ubc4p, Ubc5p (9), and likely Ubc1p (12), acting together with the *hect* domain-containing E3 activity Rsp5p [Y. Feng and N. Davis, unpublished results (3)]. While it is clear that the attached ubiquitin serves as the sufficient trigger for Ste3p internalization (5), the

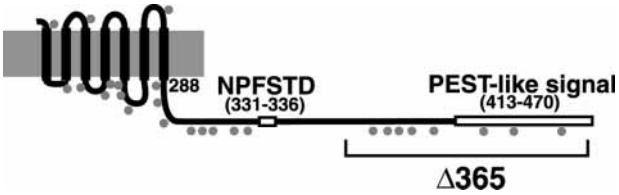

Figure 1: Ste3p schematic indicating the position of the sequences that drive both constitutive (PEST-like signal) and ligand-dependent endocytosis (NPFSTD) as well as the positions of all lysines (gray dots). The amino acid residue numbers of these key sequences are indicated. The bracketed region below indicates the sequences deleted by the Δ365 mutation.

details of how uptake is effected remain uncertain, though it is clear that the actin cytoskeleton has some critical and central participation (13).

As with other examples of ubiquitin-dependent uptake in yeast, the consequence of the Ste3p constitutive endocytosis is delivery of the receptor to the vacuole/lysosome for degradation by the resident proteases (14). As a result, in resting cells unchallenged by ligand, the mating pheromone **a**-factor, Ste3p is a short-lived protein, with a half-life of only 20 min in cells growing at 30 °C (14). This correlation, for Ste3p and for other yeast surface proteins, of ubiquitin-dependent uptake with vacuolar degradation, suggests the possibility that in addition to triggering uptake, the ubiquitin signal might also be utilized at post-surface steps to direct traffic to the vacuole.

The second Ste3p uptake mode, the ligand-dependent mechanism, was revealed by Ste3p mutants disabled for rapid constitutive endocytosis. Mutant Ste3 proteins that lack either the three lysyl ubiquitin acceptor sites, or the PEST-like signal altogether, accumulate at the surface of unstimulated cells, but are induced to undergo endocytosis when the cells are presented with the receptor ligand, the farnesylated peptide **a**-factor (5,14). This uptake utilizes a different receptor signal which includes the CTD hexapeptide sequence NPFSTD as a required feature (Figure 1) (15). NPF tripeptide sequences are known binding ligands for proteins with EH (Eps15 homology) domains (16,17); of the five yeast EH domain proteins, three, namely End3p, Pan1p, and Ede1p, show participation in endocytosis (18–20). In addition to relying on different receptor signals, the Ste3p ligand-dependent uptake mechanism also relies to some extent on different *trans*-acting endocytic components. Ste3p ligand-dependent uptake does not require the Yck1p/Yck2p casein kinases or Akr1p (11,21). Nonetheless, like all other uptake mechanisms described to date in yeast, the actin cytoskeleton appears to be required for Ste3p ligand-dependent uptake, as uptake is blocked in both *end4–1* and *end3Δ* cells (11,22), mutants which disable endocytosis apparently through disruption of the actin cytoskeleton (23–25).

Unlike the degradative outcome associated with constitutive uptake, we have recently found that the main fate associated with receptor internalized into the Ste3p ligand-dependent pathway is recycling: the bulk of receptor internalized by this mechanism is returned to the plasma membrane, while a more minor component is routed onward to the vacuole/lysosome for degradation (22). While initial examples of yeast endocytosis were found to couple to vacuolar transport and degradation, there has been a recent appreciation of a prominent role for recycling pathways which provide a trafficking connection of endosomal compartments back to the plasma membrane (22,26–28). Indeed, a recent analysis of bulk endocytic membrane flow in yeast indicates that a major fraction of membrane internalized from the cell surface rapidly recycles back to the surface, with the onward endocytic flow to the vacuole constituting a more minor component (28).

Given the central role played by ubiquitin in the degradative endocytosis associated with Ste3p constitutive uptake and the internalization of other yeast plasma membrane proteins, we were interested to examine the role of ubiquitin in the Ste3p recycling endocytic mode. Our previous work had shown that Ste3p ligand-dependent endocytosis is at least temporally associated with a ligand-dependent ubiquitination of the receptor (9). Is this ubiquitination used for triggering uptake or does it instead play some novel role in the Ste3p recycling mechanism?

Results

We have made use of *doa4Δ* mutants to investigate the role of receptor ubiquitination in the two Ste3p uptake modes. Doa4p is one of the 17 yeast deubiquitinating enzymes (29). By disassembling multiubiquitin chains to constituent monomers, these enzymes promote ubiquitin reutilization. In *doa4* mutants, free ubiquitin levels are reduced (deficient ubiquitin reutilization) and, as a consequence, ubiquitin-dependent processes, i.e. proteosome-mediated proteolysis and ubiquitin-dependent endocytosis, are impaired (4,7,8,30–32).

Effects of doa4Δ on Ste3p constitutive endocytosis

We have first examined the effect of *doa4Δ* on the ubiquitin-dependent constitutive endocytosis of Ste3p. Our previous work demonstrated that rapid constitutive ubiquitination, uptake, and turnover of Ste3p depend both upon the cytoplasmic pool of free ubiquitin and upon the two functionally redundant ubiquitin conjugating enzymes, Ubc4p and Ubc5p (9). Thus, it is not surprising to find that Ste3p constitutive ubiquitination and turnover are both substantially impaired in *doa4Δ* cells (Figure 2A,B). Indeed, the *doa4Δ* blockade of Ste3p rapid turnover has been reported previously (32). Consistent with impaired turnover being a consequence of the reduced pool of available ubiquitin, the *doa4Δ* turnover defect is reversed through a compensatory over-expression of ubiquitin from the *CUP1* promoter (Figure 2C). To identify the endocytic transport step at which the *doa4Δ* turnover blockade is instigated, we have assessed receptor localization in *doa4Δ* cells using our standard whole-cell protease-shaving protocol (5,9,10,14,22), in which intact cells are 'shaved'

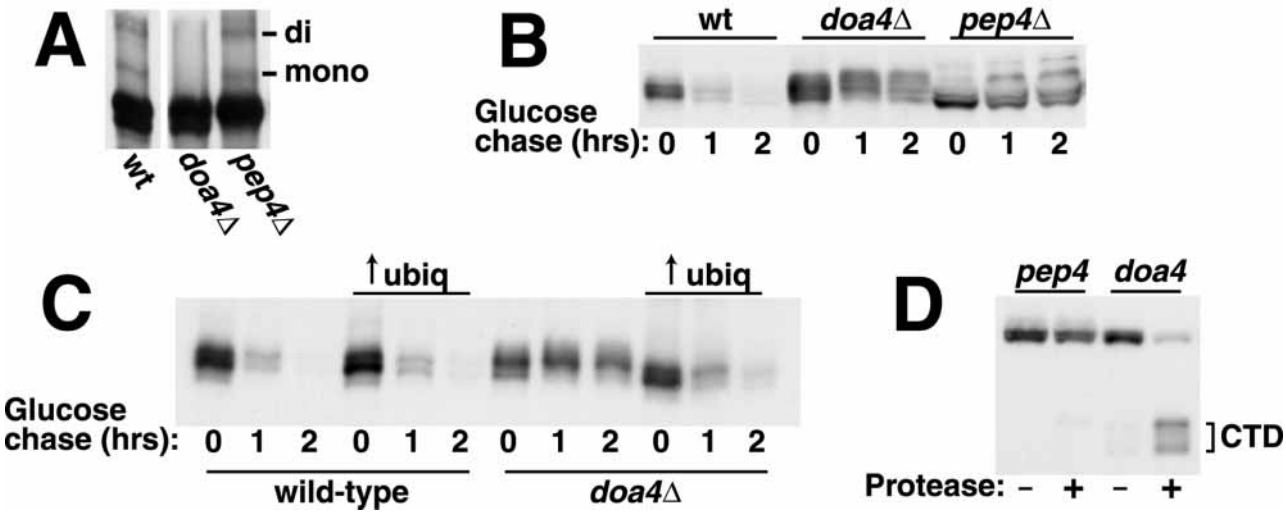

Figure 2: *DOA4* is required for the constitutive internalization of Ste3p. Ste3p expression was induced with galactose addition (2%) to *GAL1-STE3* cells that were either *doa4Δ* (NDY1241), *pep4Δ* (NDY356), or wild-type (NDY341). Following addition of glucose (3%) to repress further *GAL1*-driven Ste3p synthesis, culture aliquots were removed and treated as described below. In each case, Ste3p was visualized by Western blotting with Ste3p-specific antibodies. (A) Impaired Ste3p ubiquitination in *doa4Δ* cells. Culture aliquots were harvested immediately following 3 h of galactose-induced Ste3p expression. Protein extracts were prepared and were treated with phosphatase (see Materials and Methods) to eliminate the electrophoretic heterogeneity that results from heterogeneous phosphorylation. In order to normalize Ste3p amounts, phosphatased extracts from the *pep4Δ* cells were diluted 2.5-fold relative to the other two samples prior to gel electrophoresis. (B) Impaired Ste3p turnover in *doa4Δ* cells. At the zero timepoint, glucose was added to the three cultures, terminating a 2-h period of galactose-induced Ste3p expression. At the times indicated, culture aliquots were removed and the amount of Ste3p remaining was determined by Western blotting. (C) Overproduction of ubiquitin suppresses the Ste3p turnover defect of *doa4Δ* cells. *GAL1-STE3* cells or *GAL1-STE3 doa4Δ* cells, transformed by either the *CUP1*-ubiquitin plasmid pND186 (10) or the empty vector control plasmid YEp24(2μ/*URA3*), were cultured as described for panel C except that 1 h prior to the addition of glucose to the cultures, $CuSO_4$ was added to 100 μM, inducing high-level ubiquitin expression. (D) Ste3p endocytosis in *doa4Δ* cells is blocked at the initial cell surface internalization step. Following a 2-h period of galactose-induced expression and a subsequent 1.5-h period of glucose 'chase', culture aliquots were removed and Ste3p localization was assessed via protease shaving of the intact cells (see Materials and Methods). The electrophoretic position of a membrane-protected Ste3p fragment corresponding to the CTD and the seventh transmembrane domain is indicated at right by the brackets.

with proteases, added extracellularly. Receptor that localizes to the cell surface at the time of protease addition is digested, while receptor that localizes intracellularly is protected. For this experiment, a 2-h 'pulse' of Ste3p synthesis induced from the *GAL1* promoter was followed by an additional 1.5 h 'chase' period in which synthesis is shut off with addition of glucose to the cultures. Cells were then removed from culture and subjected to the protease shaving protocol. In *pep4Δ* cells, internalized receptor accumulates intracellularly in the vacuole (14). Consistent with such an intracellular location, receptor is found to be wholly protected from the extracellular proteases following the 1.5 h chase period (Figure 2D). A different result is seen for the receptor which accumulates in the *doa4* cell; in this context, receptor remains largely susceptible to the protease shaving, indicated both by the loss of the full-length receptor protein, and by the appearance of a characteristic digestion product corresponding to the protected, cytosolic C-terminal domain (CTD; Figure 2D). We conclude that in *doa4* cells Ste3p mainly accumulates at the cell surface, indicating that the *doa4* blockade to constitutive endocytosis is exerted at the cell surface uptake step. Thus, the *doa4* reduction to the free ubiquitin pool leads to reduced Ste3p ubiquitination and hence, reduced uptake.

Effects of doa4Δ on Ste3p ligand-dependent endocytosis

We have applied this same panel of experiments to the mechanistically distinct, ligand-dependent endocytic mode (Figure 3). To follow ligand-dependent endocytosis, we have made use of the Ste3Δ365 truncation mutant, which removes the C-terminal 105 residues of the CTD including the PEST-like signal for constitutive endocytosis (Figure 1) (10). Though fully defective for constitutive endocytosis, Ste3Δ365p remains competent for the ligand-dependent recycling mode of endocytosis (14,22): in the absence of **a**-factor ligand, Ste3Δ365p stably accumulates at the plasma membrane; with **a**-factor addition, uptake is induced. While recycling is the dominant outcome for receptor internalized into this pathway, a minority of the internalized receptor population is routed from endosomes onward to the vacuole (22). Thus, a slow *PEP4*-dependent turnover of the receptor also is associated with prolonged **a**-factor exposure.

First, we have examined the effect of the *doa4Δ* mutation on the ligand-induced ubiquitination of the receptor. We have previously found that there is clear ubiquitination of Ste3Δ365p associated (at least temporally) with its ligand-

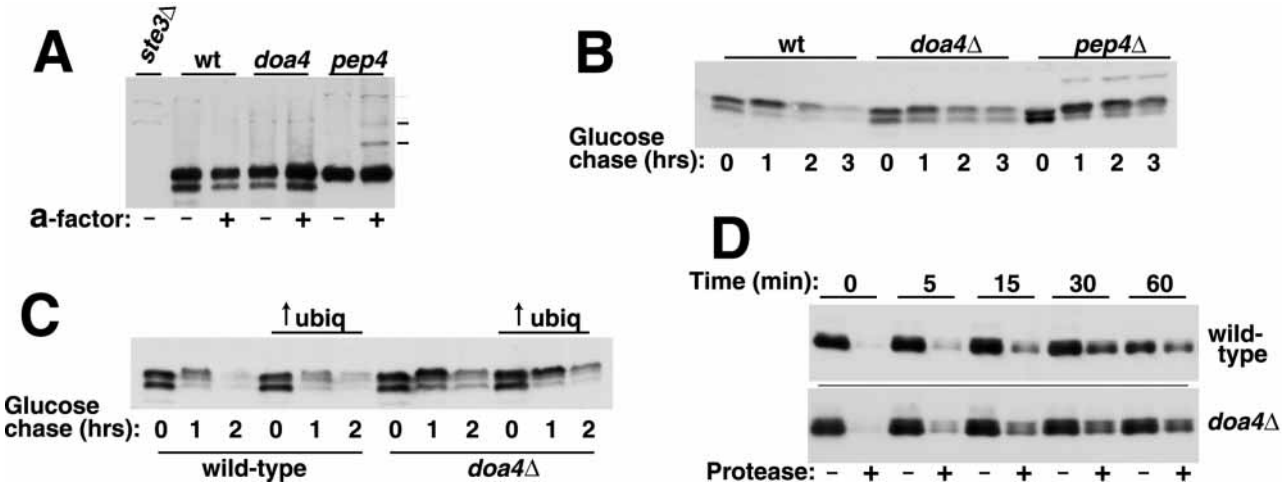

Figure 3: Effects of the *doa4Δ* mutation on the ligand-dependent endocytosis of Ste3Δ365p. A 2-h period of Ste3Δ365p expression from *GAL1-STE3Δ365* cells that were also either *doa4Δ* (NDY1219), *pep4Δ* (NDY358), or wild-type (NDY349) was induced with galactose addition (2%) to the growing cultures and was terminated by the addition of glucose (3%). Following 30 min of glucose chase, **a**-factor (see Materials and Methods) was added to induce endocytosis. At the indicated times, culture aliquots were removed and were treated as described below. Ste3Δ365p was visualized by Western blotting with Ste3p-specific antibodies. (A) Impaired Ste3Δ365p ubiquitination in *doa4Δ* cells. Following a 45-min period of **a**-factor treatment, culture aliquots were harvested and protein extracts were prepared and treated with phosphatase (see Materials and Methods). To normalize Ste3Δ365p amounts, the wild-type sample was 2-fold diluted and the *pep4Δ* sample was diluted 3-fold. The hash marks at the right indicate the electrophoretic positions of mono- and di-ubiquitinated Ste3Δ365p. (B) Effect of *doa4Δ* on ligand-induced Ste3Δ365p turnover. At the indicated times following **a**-factor addition, culture aliquots were harvested, protein extracts were prepared and analyzed for Ste3Δ365p content by Western blotting. (C) Effect of ubiquitin overproduction on the ligand-induced turnover of Ste3Δ365p in wild-type and *doa4Δ* cells. Wild-type and *doa4Δ* cells transformed by either the *CUP1*-ubiquitin plasmid pND186 (10) or the empty vector control plasmid YEp24(2μ/*URA3*) were cultured as described above, except that 100 μM $CuSO_4$ was added to the culture 30 min prior to the addition of glucose. At the indicated times following **a**-factor addition, culture aliquots were harvested, protein extracts were prepared and analyzed for Ste3Δ365p content by Western blotting. (D) Ligand-induced internalization of Ste3Δ365p is undiminished in *doa4Δ* cells. At the indicated times following **a**-factor addition to the cultures, culture aliquots of wild-type and *doa4Δ* cells were harvested and subjected to the protease-shaving regimen (see Materials and Methods).

induced endocytosis (9). In the *pep4Δ* cell context, **a**-factor challenge results in mono- and di-ubiquitination of Ste3Δ365p (Figure 3A) (9). Again, as with Ste3p constitutive endocytosis, only a minority of the total receptor population (10–15%) is found to be ubiquitinated at any time. One striking difference with the constitutive ubiquitination of Ste3p, is the requirement for the cells to be *pep4Δ* to visualize this ubiquitination: while Ste3p constitutive ubiquitination is apparent in both the *PEP4*$^+$ and *pep4Δ* cell contexts (Figure 2A); the ligand-dependent ubiquitination of Ste3Δ365p is seen only in *pep4Δ* cells, not in *PEP4*$^+$ cells (Figure 3A). This implies that for the ligand-dependent mechanism, ubiquitinated receptor is rapidly lost to vacuolar degradation, suggesting the possibility that ubiquitin may be used primarily at a late endocytic transport step, perhaps for endosome to vacuole transport. Consistent with this possibility, we have also found that *end* mutants which block both Ste3p endocytic pathways at the initial surface uptake step, have quite different effects on constitutive vs. ligand-dependent ubiquitination: while constitutive ubiquitination proceeds for Ste3p trapped at the plasma membrane by *end* mutants (9,11), the **a**-factor-induced ubiquitination of Ste3Δ365p is largely blocked in *end4–1 pep4Δ* cells (L. Chen and N. Davis, unpublished), again suggesting that ubiquitin may be used primarily at some post-surface transport step of the ligand-dependent pathway.

As a first test of the role of this ligand-induced ubiquitination in the ligand-dependent endocytic mechanism, we have examined the effect of the *doa4Δ* mutation on the slow ligand-dependent turnover of Ste3Δ365p (Figure 3B). Ste3Δ365p turnover, we find, is somewhat less efficient in *doa4Δ* cells than in wild-type cells. Nonetheless, when compared to the turnover-blocked *pep4Δ* cells, it is clear that substantial receptor turnover still does occur in the *doa4Δ* cells (Figure 3B). To test if this partial turnover defect is a reflection of the reduced ubiquitin pool in *doa4Δ* cells, again we have examined the consequence of ubiquitin overproduction. Somewhat surprisingly, we found that the partial *doa4Δ* defect was not fully reversed by ubiquitin overproduction: Ste3Δ365p turnover remains slower in *doa4Δ* cells than in wild-type cells (Figure 3C). Finally, we have examined the effects of the *doa4Δ* mutation on the kinetics of the ligand-induced internalization of Ste3Δ365p (Figure 3D). For this experiment, a pulse of Ste3Δ365p synthesis was induced from the *GAL1* promoter – first, transcriptional induction with galactose addition and then repression by subsequent glucose addition. **a**-factor was then added to induce

endocytosis and at various times thereafter, aliquots were removed from both the wild-type and *doa4Δ* cell cultures, and cells were subjected to the protease shaving protocol in order to access surface residency of the receptor. Prior to the **a**-factor challenge, all of the receptor protein in both the wild-type and the *doa4Δ* cells is found to reside at the cell surface, indicated by the full susceptibility to the added, extracellular proteases (Figure 3D). At increasing times following **a**-factor addition, an increasing proportion of the receptor population becomes resistant to digestion by the extracellular proteases, consistent with the relocalization of the receptor to the cell interior (Figure 3D). Significantly, the kinetics of this uptake in *doa4Δ* and in wild-type cells appears to be roughly equivalent (Figure 3D). Thus, while some partial effect of the *doa4Δ* mutation is apparent on Ste3Δ365p turnover (Figure 3B), the uptake step of endocytosis appears to be unaffected by the *doa4Δ* mutation. In this regard, the ligand-dependent uptake mechanism differs quite strikingly from the constitutive mechanism where Ste3p uptake was fully blocked by the *doa4Δ* mutation (Figure 2D). The implication is that uptake into the Ste3p ligand-dependent pathway may be ubiquitin-independent.

Mutation of receptor ubiquitination sites

The effect of the *doa4Δ* mutation on the cellular ubiquitin pool is a partial one; levels of free ubiquitin are reduced, not eliminated (8,31). Therefore, the possibility remained that the undiminished Ste3Δ365p internalization seen for *doa4* cells (Figure 3D) could reflect an efficient utilization of the low levels of ubiquitin that remain in these cells. To address this possibility and also to further investigate the potential involvement of ubiquitination in receptor turnover (suggested by the partial turnover defect of *doa4Δ* cells) (Figure 3B), we have constructed mutant Δ365 receptor proteins that eliminate potential ubiquitin acceptor sites from the receptor protein. Ubiquitin is attached to substrate through a pseudo-peptide linkage of the C-terminal ubiquitin carboxylic acid to the ε-amino group of substrate lysine residues. Ste3Δ365(8K→R)p has the eight lysines of the residual 77-residue-long Δ365 CTD mutated to arginine (Figure 1). Like *STE3Δ365*, the *STE3Δ365(8K→R)* allele fully restores wild-type mating function to a *ste3Δ MATα* cell (data not shown). We first tested Ste3Δ365(8K→R)p for **a**-factor-induced ubiquitination (Figure 4A). For the unsubstituted Ste3Δ365p, a low constitutive ubiquitination is apparent on receptor isolated from cells untreated with **a**-factor: both mono- and di-ubiquitinated receptor species are apparent (Figure 4A). Pheromone treatment results in a clear increase in the fraction of receptors that are ubiquitin-modified, most of the increase being mono-ubiquitinated receptor (Figure 4A). In contrast, for Ste3Δ365(8K→R)p, no ubiquitinated receptor is apparent either prior or subsequent to **a**-factor treatment. Thus, the eight Lys-to-Arg substitutions abolish ubiquitination, presumably through elimination of ubiquitin acceptor sites.

Next, we used the 8K→R receptor to address the role of receptor ubiquitination in its ligand-induced trafficking. Does the ligand-dependent ubiquitination of Ste3Δ365p function in uptake, in vacuole delivery, or in the recycling of receptor back to the plasma membrane? Effects on ligand-dependent uptake and on the slow turnover associated with this pathway were gauged as per the experiments of Figure 3, comparing the kinetics of Ste3Δ365(8K→R)p uptake and turnover to those of Ste3Δ365p (Figure 4B,C). No effect of the 8K→R mutations can be discerned on either process. To analyze the effects of the 8K→R mutations on recycling, we have utilized a protocol developed in our prior work: internalization of the Δ365 receptor is induced by **a**-factor, and then following removal of the **a**-factor ligand from the culture medium, the recycling return of receptor to the plasma membrane is followed using our standard protease-shaving protocol (22). For both Ste3Δ365p and Ste3Δ365(8K→R)p, approximately 50% of the receptor protein was found to be internalized, following a 45-min treatment with **a**-factor (Figure 3D). Our previous work indicated that when the presence of the ligand is maintained in the culture medium, the receptor population reaches a trafficking equilibrium in which continued internalization of the receptor is balanced by its recycling return to the plasma membrane (22). When ligand is withdrawn from the system, continued internalization terminates, and the recycling return to the plasma membrane of the internalized portion of the receptor population can be directly visualized (22). Comparing Ste3Δ365(8K→R)p and Ste3Δ365p in this recycling protocol, we can discern no difference in terms of the kinetics of the return of the internalized receptor back to the cell surface: i.e. following the removal of **a**-factor from the cultures, the two receptors regain susceptibility to the extracellular proteases with roughly equivalent kinetics (Figure 4D).

Thus, all three aspects of receptor trafficking within the ligand-dependent endocytic pathway, i.e. uptake, recycling and slow vacuolar turnover, appear to be unaffected by the 8K→R mutations. To eliminate the possibility that some transient ubiquitination of the receptor may still be occurring, we have constructed another receptor mutant Ste3Δ365(15K→R)p, which in addition to the 8K→R mutations, also has Lys-to-Arg substitutions of the seven lysine residues that map to the cytoplasmically disposed loops of the receptor (Figure 1). We were somewhat concerned that these additional mutations which map into the receptor core domain might disrupt receptor function: e.g. ligand-binding, G-protein-coupling, proper folding or transport to the cell surface via the secretory pathway. In qualitative tests of mating efficiency the *STE3Δ365(15K→R)* allele was found to fully complement *ste3Δ* (data not shown), indicating that the function is largely preserved for the mutant receptor. Nonetheless, assessments of the rate at which the newly synthesized receptor is delivered to the cell surface (utilizing the protease-shaving protocol) indicated that Ste3Δ365(15K→R)p traversed the secretory pathway somewhat more slowly than did Ste3Δ365p (data not shown). To compensate for this, experiments involving Ste3Δ365(15K→R)p had the glucose chase period extended; following a 2-h galactose-induced expression

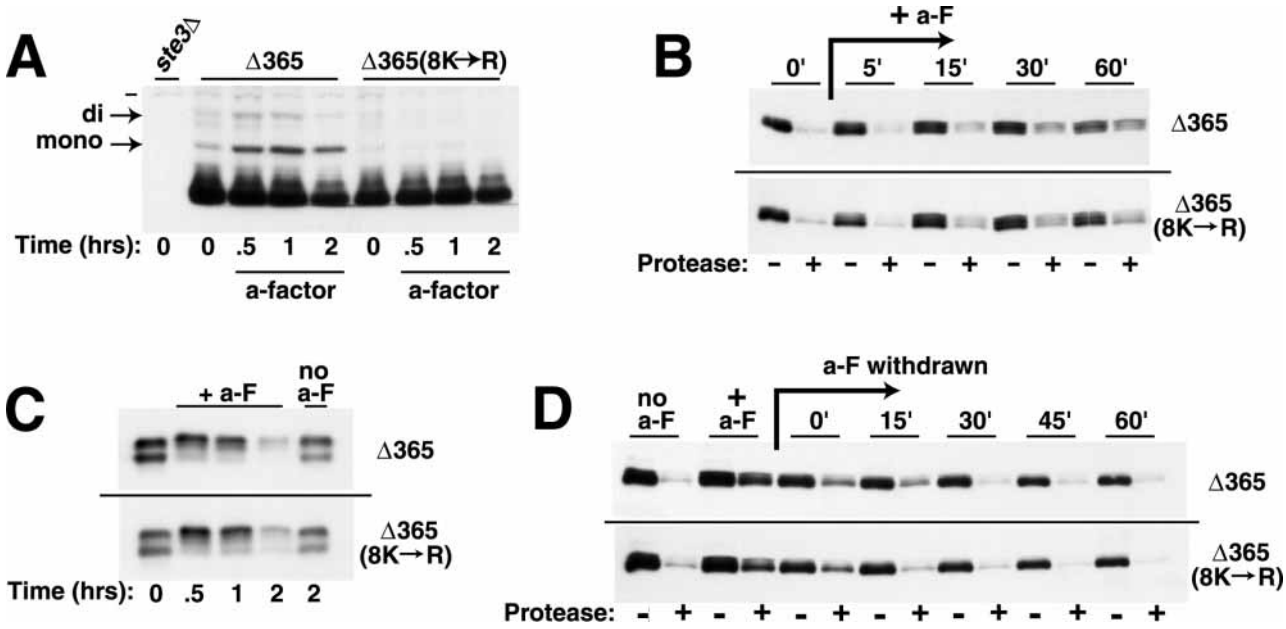

Figure 4: No effect of the 8K→R mutations on uptake, recycling, or turnover within the Ste3p ligand-dependent endocytic pathway. The ligand-dependent ubiquitination and endocytosis of Ste3Δ365p and Ste3Δ365(8K→R)p are compared. For each of the experiments below, cells were cultured for *GAL1*-driven receptor expression as described for Figure 2 and receptor protein was visualized by Western blotting with Ste3p-specific antibodies. (A) Effect of the 8K→R mutations on **a**-factor-induced receptor ubiquitination. At the indicated times following **a**-factor addition, culture aliquots of *GAL1-STE3Δ365 pep4Δ* cells (NDY358) or of *GAL1-STE3Δ365(8K→R) pep4Δ* cells (NDY1310) were harvested, protein extracts were prepared and then treated with phosphatase (see Materials and Methods) prior to gel electrophoresis. The previously determined electrophoretic positions of mono- and di-ubiquitinated Ste3Δ365p (9) are indicated by the arrows to the left. The hash mark at left indicates the position of a protein that cross-reacts with the Ste3p antibodies: this band is also present in extracts from the *ste3Δ* control cells which were processed in parallel for this experiment. (B) The ubiquitination-deficient 8K→R receptor shows unimpaired ligand-dependent uptake. At the indicated times following **a**-factor addition, *GAL1-STE3Δ365* (NDY349) or *GAL1-STE3Δ365(8K→R)* (NDY1309) cells were harvested and subjected to the protease-shaving regimen (see Materials and Methods). (C) The ubiquitination-deficient 8K→R receptor shows undiminished turnover. Receptor content was assessed by Western blotting of extracts prepared from culture aliquots of *GAL1-STE3Δ365* (NDY349) or *GAL1-STE3Δ365(8K→R)* (NDY1309) cells, harvested at the times indicated following treatment with **a**-factor or following mock pheromone treatment (no **a**-F). (D) Recycling is unimpaired for the ubiquitination-deficient 8K→R receptor. Following a 45-min treatment of *GAL1-STE3Δ365* (NDY349) or *GAL1-STE3Δ365(8K→R)* (NDY1309) cells with **a**-factor (+ **a**-F), **a**-factor was withdrawn from the cell cultures (see Materials and Methods) and the return of internalized receptor to the cell surface was followed by protease shaving (see Materials and Methods).

period (terminated by glucose addition), the time period preceding **a**-factor addition was extended from the usual 30 min to 1 h, allowing for a greater proportion of the newly synthesized Ste3Δ365(15K→R)p to reach the cell surface.

First, we examined the capacity of Ste3Δ365(15K→R)p for ligand-induced uptake (Figure 5A). Like the 8K→R receptor, the 15K→R receptor was internalized with kinetics indistinguishable from the unsubstituted Ste3Δ365p (Figure 5A). As Ste3Δ365(15K→R)p lacks any ubiquitin acceptor sites, we conclude that uptake via the Ste3p ligand-dependent endocytic mechanism does not depend on *cis*-ubiquitination of the receptor protein. To address whether the ligand-induced ubiquitination might instead be devoted to the downstream endocytic trafficking to the vacuole, we examined the effect of the 15K→R mutations on **a**-factor-induced receptor turnover. Again here, as with the 8K→R receptor, we are unable to observe any clear effect on the rate at which Ste3Δ365(15K→R)p is degraded relative to Ste3Δ365p (Figure 5B). Thus, we conclude that ubiquitination does not influence the rate at which the Δ365 receptor is delivered to the vacuole. This conclusion is somewhat at odds with the partial turnover defect observed for Ste3Δ365p in *doa4Δ* cells (Figure 3B). The finding that this *doa4* turnover defect is not suppressed by ubiquitin overproduction (Figure 3C), indicates that it is not due to a *doa4*-mediated depletion of the ubiquitin pool. Instead, the partial turnover defect could indicate some direct action of Doa4p on the vacuolar transport of Ste3Δ365p. In this regard, a recent report indicates that Doa4p acts directly upon ubiquitinated endocytic substrates, as they traverse the late endocytic pathway (33).

A C-terminal fragment is proteolytically released from the 8K→R receptor in vivo

In terms of uptake, recycling, and turnover, elimination of ligand-induced ubiquitination of Ste3Δ365p is without discernible consequence. One curious difference between Ste3Δ365(8K→R)p and Ste3Δ365p was noted, however. In

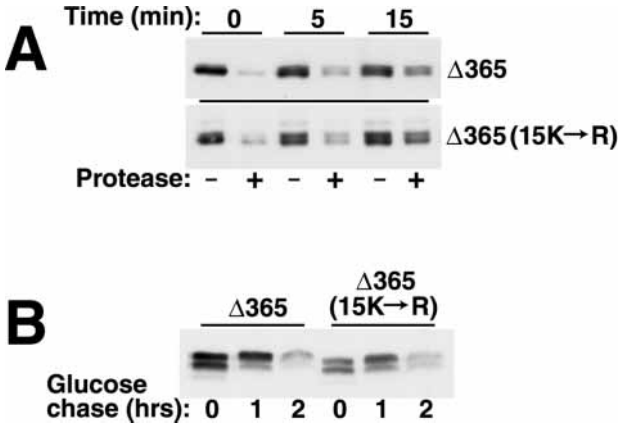

Figure 5: The 15K→R Lys-to-Arg receptor substitution mutations do not affect the kinetics of ligand-induced internalization or turnover. *GAL1-STE3Δ365* (NDY349) or *GAL1-STE3Δ365(15K→R)* (NDY1478) cells were cultured as described for Figure 2, except that the glucose chase period prior to **a**-factor treatment was increased from 30 min to 1 h to allow a greater fraction of the 15K→R mutant receptor population to reach the plasma membrane. Receptor is visualized for these experiments by Western blotting with Ste3p-specific antibodies. (A) Receptor ubiquitination is not required for the uptake step of ligand-dependent endocytosis. At the indicated times following **a**-factor addition, culture aliquots were harvested and subjected to the protease-shaving protocol, then gel electrophoresis and Western blotting. (B) Ubiquitination of the receptor is not required for its slow ligand-dependent turnover. At the indicated times following the addition of **a**-factor, culture aliquots were harvested and protein extracts were prepared for Western blotting.

the protease-shaving protocol, a diagnostic feature of successful extracellular proteolysis of surface-localized receptor is the generation of a membrane-protected Ste3 CTD fragment resulting from proteolytic clipping within the exposed, third extracellular loop. Indeed, in the absence of **a**-factor, where both Ste3Δ365p and Ste3Δ365(8K→R)p are localized fully to the plasma membrane, protease shaving results in near complete conversion of surface-localized receptor to the CTD fragment (Figure 6A). [Other receptor fragments derived from this shaving, e.g. N-terminal receptor fragments, are not visualized because the Ste3-specific antibodies used for this detection were raised exclusively against a Ste3 CTD

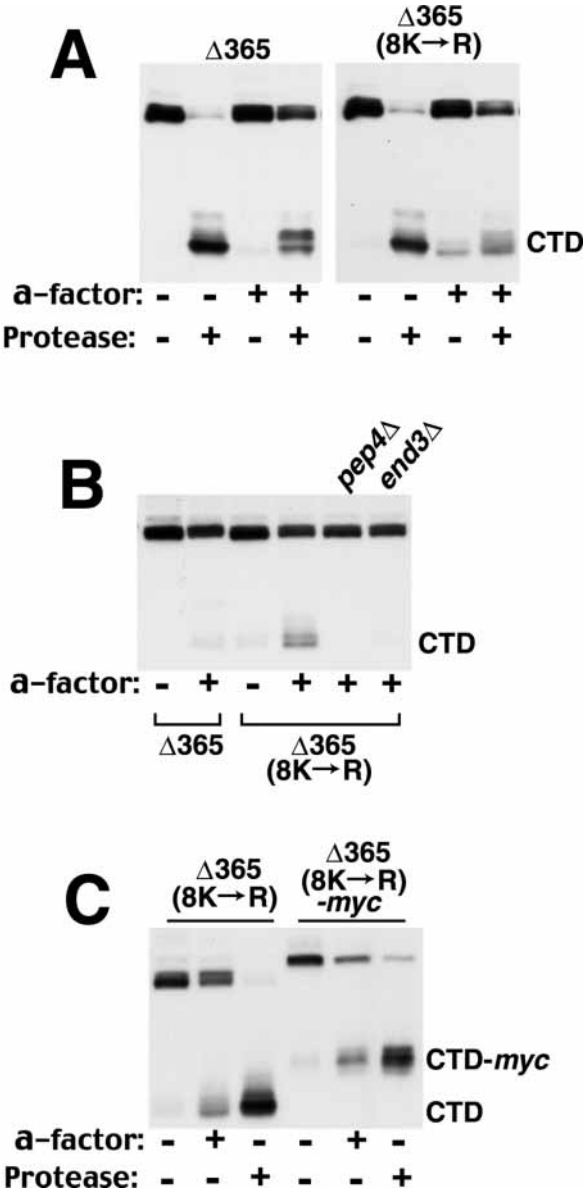

Figure 6: A proteolytic fragment associated with Ste3Δ365(8K→R)p endocytosis. Cells were cultured for *GAL1*-driven receptor expression and then 'chased' with glucose for an additional 30 min as described for Figure 2. Receptor proteins were visualized by Western blotting with Ste3p-specific antibodies. The position of Ste3-derived protein fragments are indicated to the right of each panel (CTD). (A) **a**-factor treatment results in the production of a receptor fragment from Ste3Δ365(8K→R)p that comigrates with the CTD fragment produced by protease shaving of surface-localized receptor. Localizations of Ste3Δ365p and of Ste3Δ365(8K→R)p in NDY349 and NDY1309 cells, respectively, were assessed by protease-shaving immediately prior to, or following a 45-min treatment with **a**-factor. (B) The **a**-factor-dependent 8K→R CTD fragment is C-terminal. Cells expressing either Ste3Δ365(8K→R)p (NDY1309) or Ste3Δ365(8K→R)-(*myc*)p (NDY1450), which has an additional 18-residue sequence, including the *myc* epitope, appended to the C-terminal end of the truncated Δ365 receptor, were treated with **a**-factor or proteases as described for panel A. The added epitope tag results in reduced electrophoretic mobility both for undigested receptor and for the C-terminal proteolytic fragment (CTD-*myc*). (C) The **a**-factor-induced generation of the Ste3Δ365(8K→R)p-derived CTD fragment depends on endocytosis and on vacuolar proteolytic activity. *GAL1-STE3Δ365* (NDY349), *GAL1-STE3Δ365(8K→R)* (NDY1309), *GAL1-STE3Δ365(8K→R) pep4Δ* (NDY1310), and *GAL1-STE3Δ365(8K→R) end3Δ* (NDY1482) cells were cultured, challenged with **a**-factor (+) or not (–), and then cells were collected and processed as for the no protease control samples of panel A (i.e. no extracellular proteases added).

antigen (14)]. With 45 min of **a**-factor treatment, the receptor populations are, as expected, found to be divided between surface and intracellular locales; the intracellular subpopulation resists digestion, while the portion which remains at the surface is proteolyzed, giving rise to CTD digestion product. Curiously, in the no-protease control sample of the **a**-factor-treated Ste3Δ365(8K→R)p-expressing cells but not in the parallel sample from the Ste3Δ365p cells, a Ste3 fragment is seen which corresponds roughly in size to the CTD digestion product generated by protease shaving (Figure 6A). To ascertain the identity of this **a**-factor-induced fragment, we have modified the Ste3Δ365(8K→R)p gene to encode a receptor with an additional 18 residues including the *myc* epitope tag fused at the C-terminus. The added peptide sequences retard the gel electrophoresis both of the full-length receptor protein and of the C-terminal shaving product (Figure 6B). The **a**-factor-induced fragment from these Ste3Δ365(8K→R)-(*myc*)p-expressing cells shows the same retarded gel mobility as the fragment produced by protease shaving (Figure 6B). This indicates that, like the shaving product, this fragment also is C-terminal. Extrapolating further, the fact that both the fragment generated by shaving and the fragment induced by **a**-factor treatment are C-terminal and are of similar molecular weight indicates that both also share similar N-terminal endpoints, likely generated in both cases by clipping within the same third extracellular loop domain. For the protease-shaving experiment, proteolysis of the surface-localized receptor within the extracellular oriented loop domains is expected. In the absence of added proteases, how might **a**-factor stimulate clipping within this same loop?

To test if the **a**-factor-induced clipping might be a consequence of the **a**-factor-induced endocytosis of the 8K→R receptor, we have examined the effect of the *end3Δ* mutation on this fragment production; *END3* function is required for uptake into both of the Ste3p constitutive and ligand-dependent endocytic pathways (11). The *end3Δ* mutation, we find, blocks CTD fragment production (Figure 6C), indicating that the **a**-factor-induced proteolysis depends upon receptor internalization into the cell, suggesting further that the responsible protease may reside intracellularly. A clue regarding the identity of the responsible protease activity comes from the additional finding that CTD fragment production is blocked in *pep4Δ* cells (Figure 6C); thus, fragment production requires vacuolar protease activity. One model that could accommodate both the need for endocytosis and vacuolar proteolytic activity would have the internalized 8K→R receptor delivered to the limiting membrane of the vacuole; receptor orientation would be expected to be such that its 'extracellular' loops would protrude into the vacuolar lumen and would thus be available for digestion by resident proteases, while 'cytoplasmic' loops would remain within the cytoplasm and thus be protected.

Ubiquitination controls vacuolar localization

For several plasma membrane polytopic integral membrane proteins, endocytosis has been shown to deliver the internalized proteins to the interior space of the vacuole, rather than to the limiting vacuolar membrane as might be expected for transport via typical vesicular trafficking mechanisms (33–37). Such proteins are thought to reach the lumens of the yeast vacuole or mammalian lysosome on small vesicles, released into the interior space through fusion of the late endosome, the multivesicular body (MVB), with the vacuole/lysosome (34,38). The preceding step, i.e. how vesicles first get internalized into the MVB lumenal space, is not yet understood.

In Figure 7, we have examined the localization in *pep4Δ* cells of HA-epitope-tagged receptors by indirect immunofluorescent microscopy following an extended 2-h treatment of cells with **a**-factor. Although recycling is the major fate for internalized Δ365 receptor, with long exposure to **a**-factor, eventually (presumably after multiple rounds of uptake and recycling), the bulk of the receptor is delivered to the vacuole where in *PEP4*$^{+}$ cells it is degraded and in *pep4Δ* cells, it is sequestered (14,22). This analysis was facilitated by a change in the yeast strain background. The strain background used for the prior experiments [derived from HR144–3D (18)] has small vacuoles (data not shown), making it difficult to distinguish if receptor is delivered to the vacuole interior or not. The strain background that we have instead used (derived from LRB757) (39) has relatively large vacuoles (Figure 7). While the two strains differ in terms of the physical presentation of the vacuoles, vacuolar function, assessed in terms of the kinetics of Ste3p turnover, is indistinguishable (data not shown). Most relevant with regard to the immunofluorescence analysis presented below (Figure 7), as was seen previously in the HR144–3D strain background (Figure 4C), Ste3Δ365(8K→R)p cannot be distinguished from Ste3Δ365p in terms of the kinetics of its ligand-induced turnover, indicating that there is no difference in the rate at which the two receptors are delivered to the vacuole.

First we have examined the endpoint localization of HA-tagged wild-type Ste3p internalized via the constitutive endocytic pathway. Localization was assessed in *pep4Δ* cells, 2.5 h subsequent to glucose-mediated repression of Ste3(HA)p synthesis from the *GAL1* promoter. Receptor staining at this timepoint was found to be wholly intracellular, the surface having been fully cleared by endocytosis (Figure 7). Receptor was visualized as discrete puncta mapping into the lumenal space of the vacuole (by Nomarski optics, the vacuole presents as an apparent depression of the cell surface; note 'composite' image having the red fluorescent signal superimposed onto the Nomarski image; Figure 7). This presentation is consistent with localization to intravacuolar vesicles. The images displayed are deconvolved cross-sections (see Materials and Methods); inspection of neighboring sections identifies additional intravacuolar puncta (not shown); on average, 5–10 puncta can be distinguished per vacuole. Thus, we conclude that Ste3p constitutive endocytosis delivers receptor-containing vesicles to the vacuole lumen.

For receptor internalized via the ligand-dependent pathway, we find that Ste3Δ365p following the 2 h **a**-factor treatment

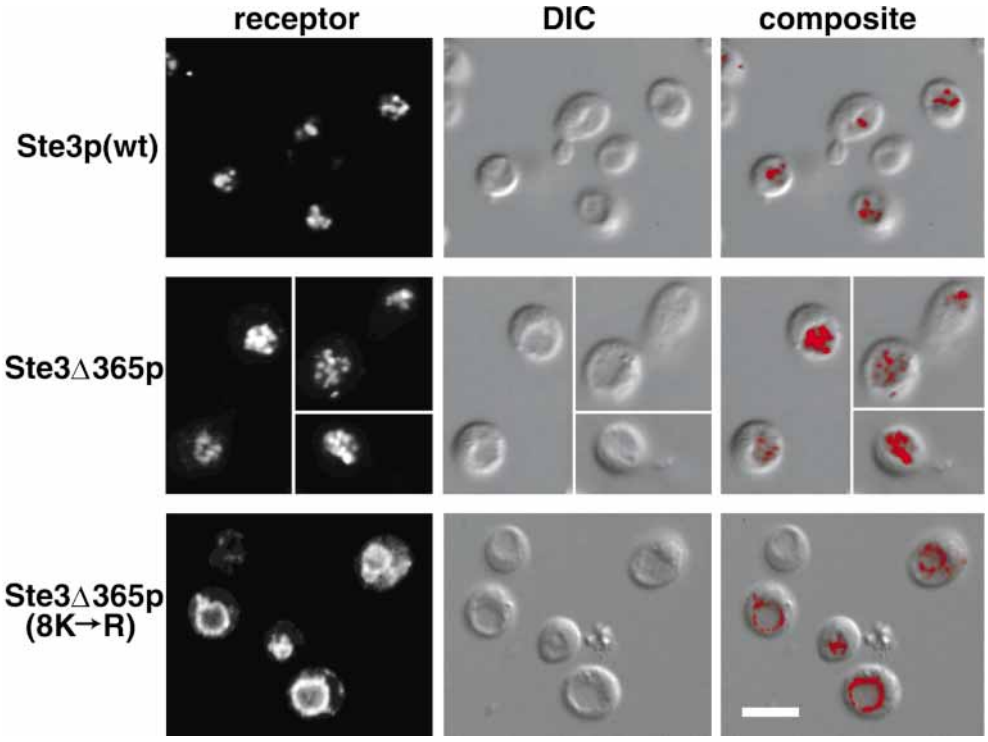

Figure 7: The 8K→R receptor is delivered to the limiting membrane of the vacuole rather than to vacuole interior. A 3-h period of galactose-induced expression of HA epitope-tagged Ste3p, Ste3Δ365p, and Ste3Δ365(8K→R)p in the *pep4Δ* strains NDY1475, NDY1457, and NDY1458, respectively, was followed by a 2.5 h glucose chase period. Ste3Δ365p- and the Ste3Δ365(8K→R)p-expressing cells had **a**-factor added for the final 2 h of the glucose chase period to induce endocytosis. Cells were prepared for immunofluorescent analysis (see Materials and Methods) and incubated with anti-HA mAb, followed by a Cy3-conjugated goat anti-mouse antibody. The panels at left are the result of computer deconvolution of the fluorescent signal at a single focal plane. The same focal plane of the same cells is imaged in the middle panels by DIC. Panels at right show a superposition of the fluorescent signal (red) overlaid onto the DIC image. A 10-μm scale bar (white) is seen in the bottom right panel.

shows an endpoint localization quite similar to that seen for wild-type receptor internalized via the constitutive pathway. Following such an extended **a**-factor treatment, receptor is again found to be exclusively intracellular, again localizing to intravacuolar puncta (Figure 7). Quite a different result was seen with the parallel analysis of internalized Ste3Δ365(8K→R)p. Rather than intravacuolar puncta, the 8K→R receptor instead appears to decorate the limiting membrane of the vacuole (Figure 7). Thus, while ligand-induced ubiquitination is not utilized to direct uptake, recycling or turnover of the receptor, it does appear to play a role in directing receptor traffic into the vacuole lumen.

Discussion

Ubiquitin-independent endocytosis

Previous work has shown that different receptor signals and to some extent, different cellular proteins are used to instigate uptake into the two Ste3p endocytic pathways (11,14,15,21). Receptor internalized into the two pathways also differs in terms of fate – constitutive uptake leads to rapid degradation in the vacuole, while the ligand-dependent mechanism couples largely to recycling (14,22). In the present work, we find another major difference in terms of the role that ubiquitin plays in the two mechanisms.

First, the *doa4Δ* mutation which reduces ubiquitin availability within the cell was found to have quite a different effect on the two uptake mechanisms. While the *doa4Δ* mutation blocked the ubiquitin-dependent, constitutive uptake of the receptor (Figure 2D), no discernible effect on the ligand-dependent uptake of Ste3Δ365p (Figure 3D) was seen. Although this could indicate that ubiquitination is not required for ligand-dependent uptake, the possibility remained that the undiminished uptake seen for *doa4Δ* cells might instead result from efficient scavenging of the low residual levels of ubiquitin that remain available in these cells. To address this possibility, Lys-to-Arg missense mutations were introduced into Ste3Δ365p to eliminate potential ubiquitination sites within the receptor protein. The 8K→R mutant removed all eight lysines from the residual Δ365 CTD (Figure 1), while the 15K→R mutant additionally removed the seven lysine residues that map to the three cytoplasmic loops of the receptor protein (Figure 1). Neither of these two Lys-to-Arg mutant receptors showed any impairment in terms of their ligand-induced internalization (Figures 4B and 5A). Thus, we feel confident in concluding that uptake into the Ste3p ligand-

dependent pathway does not require ubiquitination of the receptor and thus stands uniquely in yeast as a ubiquitin-independent uptake mechanism. Consistent with this conclusion, it has been reported recently that an NPF sequence introduced into the context of a mutant α-factor receptor (Ste2p), having all the lysine residues of the Ste2p CTD substituted by arginines, was able to restore endocytic function indicating that NPF-mediated uptake in general may be ubiquitin independent (40). However, this mutant Ste2p construct did retain the lysine residues that map to the cytosolic loops of the α-factor receptor; thus, some possibility of receptor ubiquitination remained.

Recycling – the default sorting option?

The various examples of ubiquitin-dependent uptake in yeast studied to date all lead to rapid degradation of the internalized substrate protein in the vacuole (1,2), suggesting the possibility of obligate coupling of ubiquitin-dependent uptake to vacuole-directing trafficking and turnover. It seems significant in this regard that the one example of ubiquitin-independent uptake, i.e. the ligand-dependent uptake of Ste3Δ365p described herein, is instead most prominently associated with recycling. Thus, while cell-surface ubiquitination may route the endocytic substrate to the vacuole for degradation, ubiquitin-independent uptake may couple instead into a recycling pathway. A recent report on bulk membrane flow in yeast indicates that a major fraction of membrane internalized from the cell surface rapidly recycles back to the surface, with the onward endocytic flow to the vacuole constituting a more minor component (28). In the absence of a ubiquitin signal to direct the onward transport to the vacuole, internalized receptor may simply ride the bulk flow of membrane back to the surface. In this scenario, recycling would be the default and recycling substrates would not require specialized signals to specify routing back to the surface. In this regard, it will be interesting to see if the two other yeast examples of recycling proteins, chitin synthetase Chs3p (26) and Snc1p SNARE protein (27), also are internalized via ubiquitin-independent mechanisms. Default recycling in yeast is consistent with the current understanding of recycling in mammalian cells. As in yeast, mammalian cell membrane recycling constitutes a major portion of the bulk endocytic membrane flow (41). Furthermore, it appears that the recycling of internalized receptors does not require a specialized signal, occurring instead by default (42).

Ubiquitination directs transport into the vacuole lumen

What then is the function of Ste3p ligand-induced ubiquitination? While elimination of receptor *cis*-ubiquitination does not grossly perturb the rate at which receptor is turned over, we have found that receptor ubiquitination does have a striking effect on the receptor's final vacuolar localization. This is clearly seen for the endpoint localizations of Ste3Δ365p and Ste3Δ365(8K→R)p following an extended treatment of the cells with **a**-factor (Figure 7). Ste3Δ365p, like wild-type Ste3p delivered to the vacuole via constitutive endocytosis, accumulates in punctate structures within the vacuolar interior. In contrast, Ste3Δ365(8K→R)p was found to decorate the limiting membrane of the vacuole. This finding suggests that attached ubiquitin may play a role in directing how substrate is delivered to the vacuole, i.e. whether it is delivered to the interior space of the vacuole, or alternatively, to the limiting membrane. Delivery of membrane proteins to the vacuole lumen is thought to occur through fusion of the multivesicular late endosome with the vacuole/lysosome (34,38). The multivesicular body (MVB) is a topologically complex organelle having interior vesicles contained within a limiting outer membrane. Fusion of the MVB with the vacuole/lysosome delivers the MVB lumenal vesicles into the lumen of the vacuole/lysosome, while proteins present in the MVB limiting membrane may transfer to the vacuole/lysosome limiting membrane (27,43). The punctate presentations of endocytosed Ste3p and Ste3Δ365p are consistent with localization to lumenal vacuolar vesicles. The two different endpoint localizations for ubiquitinated and non-ubiquitinated receptors point toward a role for the ubiquitin signal in directing traffic through the MVB, with active sequestration of the ubiquitinated receptor into lumenal MVB vesicles.

Our results are consistent with several recent reports that indicate a new, generalized role for ubiquitin in directing late endosomal traffic through the MVB into the vacuole lumen (37,44–46). The MVB provides a convergent trafficking step to the vacuole/lysosome, both for endocytic traffic from the plasma membrane and for biosynthetic traffic of the newly synthesized hydrolases that are delivered to the vacuole from the Golgi (14,47–49). Thus, in addition to the role of ubiquitin in sorting at the MVB for endocytic traffic to the vacuole, as indicated both by our work on Ste3p and by a prior report on the ABC transporter Ste6p (37), a similar role for ubiquitin at the MVB has now also been suggested for the biosynthetic traffic of the newly synthesized hydrolases to the vacuole lumen (44,46). In addition, there has also been exciting progress in the elucidation of the mechanism by which the ubiquitinated substrate is sequestered into the MVB lumenal vesicles – a protein complex composed of Vps23p, Vps28p, and Vps37p, apparently acts at the MVB to recognize the ubiquitinated substrates and somehow to direct sequestration into the lumenal vesicles (44).

Thus, in addition to its role in directing endocytic uptake at the plasma membrane in yeast, it is now clear that ubiquitin also is utilized to direct traffic late in the endocytic pathway through the MVB. This new role for ubiquitin likely also applies to the endocytic trafficking in mammalian cells. A late-acting function for receptor ubiquitination has also been established for the EGF and IL-2 receptors: ubiquitinated receptors are preferentially targeted for lysosomal destruction, rather than for recycling (50,51).

The Ste3p ligand-dependent endocytic pathway

Our previous work demonstrated recycling to be the primary fate of receptor internalized by the ligand-dependent uptake mechanism (22). Here, we show that the ubiquitin signal is required neither for the uptake nor for the associated recycling. From this, we extrapolate a general model in which re-

cycling is seen as the default option, i.e. sorting that does not require a specialized signal. Based upon published analysis of bulk endocytic membrane flow (28), we expect that the Ste3p recycling compartment is likely to be the early endosome. Although the receptor may normally be subject to multiple rounds of ligand-induced uptake and recycling, eventually, with prolonged exposure of the cells to **a**-factor, appreciable amounts of receptor are removed from the recycling pathway and directed onward to the MVB and vacuole for degradation; under such conditions of continuous ligand exposure, the receptor half-life for degradation is typically about 90 min (Figures 3–5) (22). Again here, ubiquitination is not required for this redirection out of the recycling pathway; the kinetics of vacuole-dependent turnover are not compromised for the non-ubiquitinatable 8K→R and 15K→R receptor mutants (Figures 3C and 4B). Indeed, it is only at the final transport step, the transit of receptor through the MVB to the vacuole, that we find a role for ubiquitination: ubiquitinated receptor being sequestered into the lumenal vesicles of the MVB and then to the vacuole lumen, while the ubiquitination-deficient 8K→R receptor is instead delivered to the vacuole limiting membrane. Consistent with a late role for ubiquitination in the ligand-dependent pathway, we are able to detect the receptor ubiquitination only in *pep4Δ* cells (Figure 3A) (in contrast to the ubiquitination associated with the constitutive endocytosis of the receptor: Figure 2A). This implies that ubiquitinated receptor species are short lived, suggesting that ubiquitination may occur just prior to the *PEP4*-dependent degradation of the receptor, perhaps added to the receptor while resident at the MVB.

Given the striking effect of ubiquitination on the vacuolar localization of the receptor, it is surprising that we detect no major difference in the kinetics of turnover for the ubiquitinated vs. the ubiquitination-deficient receptors. Apparently, receptor can be efficiently turned over even when delivered to the limiting membrane of the vacuole. Furthermore, receptor localized to this limiting membrane is not merely clipped (as is seen in Figure 6), but rather fully degraded; preliminary data indicate that the *PEP4*-dependent CTD proteolytic clipping product (Figure 6) is a relatively long-lived intermediate in the process of more complete degradation of the receptor protein (data not shown); clipped CTD products do not accumulate to significant extents in the typical ligand-dependent turnover experiments such as those shown for Ste3Δ365(8K→R)p (Figure 4C) and Ste3Δ365(15K→R)p (Figure 5B).

Our work on the Ste3p ligand-dependent endocytic pathway presents two new paradigms connecting ubiquitin and endocytosis. First, we find that receptor internalized via a ubiquitin-independent uptake mechanism recycles. Recycling, we hypothesize, may be the default sorting mechanism that occurs in the absence of the ubiquitin signal. In addition, our work provides support for an exciting new role for ubiquitin in directing traffic through the MVB, with ubiquitinated substrate being internalized into lumenal vesicles and with the non-ubiquitinated substrates being left behind at the limiting membrane.

Materials and Methods

Strains

The strains used in this work are listed in Table 1. The new strains constructed for this work were constructed using standard yeast gene replacement methodologies. Disruption of the *DOA4* and *END3* genes involved exact PCR-mediated replacement of the ORFs by the $G418^R$-conferring *kan-MX2* allele (52), essentially as previously described (11). Other strains were constructed through introduction of mutant *STE3* alleles into the

Table 1: Yeast strains

Strain	Genotype	Reference or Source[a]
EG123	*MAT***a** *ura3 leu2 trp1 his4*	(56)
NDY341	*MATα GAL1-STE3 ura3 leu2 his4 bar1–1*	(9)
NDY343	*MATα ste3Δ::LEU2*	(10); A
NDY349	*MATα GAL1-STE3Δ365*	(22); A
NDY356	*MATα GAL1-STE3 pep4Δ*	(9); A
NDY358	*MATα GAL1-STE3Δ365 pep4Δ*	(22); A
NDY372	*MATα ste3Δ::LEU2 pep4Δ*	(5); A
NDY1219	*MATα GAL1-STE3Δ365 doa4Δ::G418^R*	This work; A
NDY1241	*MATα GAL1-STE3 doa4Δ::G418^R*	This work; A
NDY1309	*MATα GAL1-STE3Δ365(8K→R)*	This work; A
NDY1310	*MATα GAL1-STE3Δ365(8K→R) pep4Δ*	This work; A
NDY1450	*MATα GAL1-STE3Δ365(8K→R)-(c-myc)*	This work; A
NDY1478	*MATα GAL1-STE3Δ365(15K→R)*	This work; A
NDY1482	*MATα GAL1-STE3Δ365(8K→R) end3Δ::G418^R*	This work; A
NDY1080	*MATα GAL1-STE3 pep4Δ ura3–52 leu2 his3*	(11)
NDY1456	*MATα ste3Δ::LEU2 pep4Δ*	This work; B
NDY1457	*MATα GAL1-STE3Δ365-(HA) pep4Δ*	This work; B
NDY1458	*MATα GAL1-STE3Δ365(8K→R)-(HA) pep4Δ*	This work; B
NDY1475	*MATα GAL1-STE3-(HA) pep4Δ*	This work; B

[a] Strains designated A are isogenic to NDY341 except as indicated. Strains designated B are isogenic to NDY1080 except as indicated.

chromosome at the *STE3* locus in place of an endogenous *ste3Δ::LEU2* allele (10) by a two-step gene replacement methodology previously described (9). The *ste3Δ::LEU2* starting strains for these constructions were NDY343 (10), NDY372 (5), and NDY1456. NDY1456 was constructed by two-step gene replacement of the *GAL1-STE3* allele of NDY1080 (11) by the *ste3Δ::LEU2* allele of pSL2165 integrating plasmid (10).

Lys-to-Arg STE3 mutant alleles

The new *STE3* alleles for chromosomal integration all were constructed from the starting point of the *GAL1-STE3* pSL1904 integrating plasmid (5). Δ365 is an in-frame deletion of sequences encoding residues 365–468 of Ste3 (14). The *GAL1-STE3Δ365(8K→R)* allele substitutes Arg codons for the eight Lys codons of the residual Δ365 CTD (Figure 1): i.e. K291R, K297R, K306R, K311R, K313R, K315R, K323R, K328R. These 8K→R Lys-to-Arg substitutions were introduced into *GAL1-STE3Δ365* plasmid on a mutated 231 bp *STE3* Nde I to Sal I restriction fragment (encoding Ste3 residues 288 through 365) generated by the PCR-based SOEing methodology (53), using three 100-mer oligonucleotides that overlapped with one another by 20 bp. The seven additional Lys-to-Arg substitutions (i.e. K29R, K99R, K102R, K105R, K185R, K186R, K188R) (Figure 1) present in the 15K→R allele were generated by separate oligonucleotide-directed mutagenesis (54) of the Lys codons present in the sequences encoding the three Ste3p cytoplasmic loops. The fidelity of the introduced mutations was confirmed through DNA sequencing of the relevant portions of the final 8K→R and 15K→R mutant plasmids.

Epitope-tagged STE3 alleles

To construct the *GAL1-STE3Δ365(8K→R)-(c-myc)* allele, the *c-myc* 9E10 epitope fused to the C-terminal sequences of a *GAL1-STE3Δ365(c-myc)* construct (14) was ligated to the C-terminal sequences of a *GAL1-STE3Δ365(8→R)* construct. With the epitope addition, 18 residues are added to the C-terminus of Ste3Δ365(8K→R)p. To construct the C-terminally HA epitope-tagged Ste3p, i.e. *GAL1-STE3-(HA)*, a DNA duplex composed of two annealed, complementary 33-mer oligonucleotides encoding a single HA epitope and having Xho I/Sal I complementary 5′ overhangs, was inserted at an Xho I restriction site previously created by oligonucleotide-directed mutagenesis (54) at *STE3* C-terminal codons 466 and 467 (5). The Xho I site re-created to the upstream side of the tag-encoding sequence of *GAL1-STE3-(HA)* was used for ligation to C-terminal Sal I sites present in both the *GAL1-STE3Δ365 and GAL1-STE3Δ365(8K→R)* constructs, generating the HA epitope-tagged versions of these alleles.

Cell culture, a-factor treatment, protein extract preparation, and Western analysis

A period of receptor expression was induced from strains carrying the various *GAL1*-driven *STE3* mutant alleles growing in YPR medium (1% yeast extract, 2% peptone, 2% raffinose) with addition of galactose to 2% and was terminated with the subsequent addition of glucose to 3%. Subsequent treatment with **a**-factor, involved the addition of a 0.5 vol of a culture supernatant from EG123 cells carrying the **a**-factor overproduction plasmid pKK16(*2μ/URA3/STE6/MFA2) (*14,55). Aliquots removed from cultures just prior to the **a**-factor treatment step (the zero timepoint), or at indicated times thereafter, were either directly processed into protein extracts or were subjected to the protease-shaving protocol. Protein extracts were prepared for SDS-PAGE and Western analysis as previously described (5).

Phosphatase treatment

Visualization of the ubiquitinated receptor forms is facilitated by reducing the heterogeneity in receptor gel mobility caused by its heterogeneous phosphorylation. For this, protein extracts were treated with potato acid phosphatase (Roche, Nutley, NJ, USA) as described (9) prior to SDS-PAGE.

Protease shaving

To assess the fraction of the receptor population residing at the cell surface, intact cells were treated with Pronase (Calbiochem-Novabiochem, San Diego, CA, USA) or mock-treated in parallel (no added protease) as previously described (14,22). Energy poisons (10 mM sodium azide, 10 mM potassium fluoride) are included during the 60-min digestion as well as during a 30-min preincubation to block the possibility of ongoing receptor trafficking. Extracts prepared through glass bead lysis of the cells into 10% trichloroacetic acid (14) were subjected to SDS-PAGE and then Western analysis.

Recycling

The recycling of internalized receptor was followed as previously described (22). In brief, following 45 min of **a**-factor treatment (which resulted in substantial internalization of the Δ365 receptor), cells were collected from culture by centrifugation, washed with fresh medium and restored to culture. The rate of recycling return of the internalized receptor back to the cell surface was then followed using the protease shaving protocol.

Indirect immunofluorescent microscopy

Cells were fixed, spheroplasted, and otherwise prepared for indirect immunofluorescent microscopy as described (14). Detection of HA-epitope-tagged receptor proteins entailed a 1-h incubation with a 1 : 1000 dilution of the HA.11 mAb (Covance, Princeton, NJ, USA) followed by a secondary 1-h incubation with a 1 : 500 dilution of a Cy3-conjugated donkey anti-mouse IgG (Jackson ImmunoResearch, West Grove, PA, USA). A z-series of digital images of the fluorescent cells collected at focal planes separated by 0.25 μm increments using a Nikon Eclipse 800 microscope equipped with epifluorescence, an ORCA II CCD camera (Hamamatsu, Bridgewater, NJ, USA), and motorized stage. Fluorescent images were deconvolved using Inovision ISee software (Inovision, Raleigh, NC, USA).

Acknowledgments

We are specially thankful to Bob Fuller, Dennis Thiele, and Dave Engelke for the use of their microscope and imaging facility, also to Hao Zhou and E. J. Brace regarding the microscopy and deconvolution instruction and advice. Finally, we thank our colleagues Amy Roth and Ying Feng for advice, insights, and encouragement throughout the course of this work. This work was supported by a grant from the National Science Foundation (MCB 99–83688).

References

1. Bonifacino JS, Weissman AM. Ubiquitin and the control of protein fate in the secretory and endocytic pathways. Annu Rev Cell Dev Biol 1998;14:19–57.
2. Hicke L. Gettin′ down with ubiquitin: turning off cell-surface receptors, transporters and channels. Trends Cell Biol 1999;9:107–112.
3. Rotin D, Staub O, Haguenauer-Tsapis R. Ubiquitination and endocytosis of plasma membrane proteins: role of Nedd4/Rsp5p family of ubiquitin-protein ligases. J Membr Biol 2000;176:1–17.
4. Terrell J, Shih S, Dunn R, Hicke L. A function for monoubiquitination in the internalization of a G protein-coupled receptor. Mol Cell 1998;1:193–202.
5. Roth AF, Davis NG. Ubiquitination of the PEST-like endocytosis signal of the yeast **a**-factor receptor. J Biol Chem 2000;275:8143–8153.
6. Shih SC, Sloper-Mould KE, Hicke L. Monoubiquitin carries a novel internalization signal that is appended to activated receptors. EMBO J 2000;19:187–198.
7. Galan J, Haguenauer-Tsapis R. Ubiquitin lys63 is involved in ubiquitin-

ation of a yeast plasma membrane protein. EMBO J 1997;16:5847–5854.
8. Springael JY, Galan JM, Haguenauer-Tsapis R, Andre B. NH4+-induced down-regulation of the *Saccharomyces cerevisiae* Gap1p permease involves its ubiquitination with lysine-63-linked chains. J Cell Sci 1999;112:1375–1383.
9. Roth AF, Davis NG. Ubiquitination of the yeast **a**-factor receptor. J Cell Biol 1996;134:661–674.
10. Roth AF, Sullivan DM, Davis NG. A large PEST-like sequence directs the ubiquitination, endocytosis, and vacuolar degradation of the yeast **a**-factor receptor. J Cell Biol 1998;142:949–961.
11. Feng Y, Davis NG. Akr1p and the type I casein kinases act prior to the ubiquitination step of yeast endocytosis: Akr1p is required for kinase localization to the plasma membrane. Mol Cell Biol 2000;20:5350–5359.
12. Hicke L, Riezman H. Ubiquitination of a yeast plasma membrane receptor signals its ligand-stimulated endocytosis. Cell 1996;84:277–287.
13. D'Hondt K, Heese-Peck A, Riezman H. Protein and lipid requirements for endocytosis. Annu Rev Genet 2000;34:255–295.
14. Davis NG, Horecka JL, Sprague GF Jr. *Cis*- and *trans*-acting functions required for endocytosis of the yeast pheromone receptors. J Cell Biol 1993;122:53–65.
15. Tan PK, Howard JP, Payne GS. The sequence NPFXD defines a new class of endocytosis signal in *Saccharomyces cerevisiae*. J Cell Biol 1996;135:1789– 800.
16. Paoluzi S, Castagnoli L, Lauro I, Salcini AE, Coda L, Fre S, Confalonieri S, Pelicci PG, Di Fiore PP, Cesareni G. Recognition specificity of individual EH domains of mammals and yeast. EMBO J 1998;17:6541–6550.
17. Salcini AE, Confalonieri S, Doria M, Santolini E, Tassi E, Minenkova O, Cesareni G, Pelicci PG, Di Fiore PP. Binding specificity and *in vivo* targets of the EH domain, a novel protein–protein interaction module. Genes Dev 1997;11:2239–2249.
18. Raths S, Rohrer J, Crausaz F, Riezman H. *end3* and *end4*. two mutants defective in receptor-mediated and fluid- phase endocytosis in *Saccharomyces cerevisiae*. J Cell Biol 1993;120:55–65.
19. Wendland B, McCaffery JM, Xiao Q, Emr SD. A novel fluorescence-activated cell sorter-based screen for yeast endocytosis mutants identifies a yeast homologue of mammalian Eps15. J Cell Biol 1996;135:1485–1500.
20. Gagny B, Wiederkehr A, Dumoulin P, Winsor B, Riezman H, Haguenauer-Tsapis R. A novel EH domain protein of *Saccharomyces cerevisiae*, Ede1p, involved in endocytosis. J Cell Sci 2000;113:3309–3319.
21. Givan SA, Sprague GF Jr. The ankyrin repeat-containing protein Akr1p is required for the endocytosis of yeast pheromone receptors. Mol Biol Cell 1997;8:1317–1327.
22. Chen L, Davis NG. Recycling of the yeast **a**-factor receptor. J Cell Biol 2000;151:731–738.
23. Holtzman DA, Wertman KF, Drubin DG. Mapping actin surfaces required for functional interactions *in vivo*. J Cell Biol 1994;126:423–432.
24. Ayscough KR, Stryker J, Pokala N, Sanders M, Crews P, Drubin DG. High rates of actin filament turnover in budding yeast and roles for actin in establishment and maintenance of cell polarity revealed using the actin inhibitor latrunculin-A. J Cell Biol 1997;137:399–416.
25. Tang HY, Munn A, Cai M. EH domain proteins Pan1p and End3p are components of a complex that plays a dual role in organization of the cortical actin cytoskeleton and endocytosis in *Saccharomyces cerevisiae*. Mol Cell Biol 1997;17:4294–4304.
26. Chuang JS, Schekman RW. Differential trafficking and timed localization of two chitin synthase proteins, Chs2p and Chs3p. J Cell Biol 1996;135:597–610.
27. Lewis MJ, Nichols BJ, Prescianotto-Baschong C, Riezman H, Pelham HR. Specific retrieval of the exocytic SNARE Snc1p from early yeast endosomes. Mol Biol Cell 2000;11:23–38.
28. Wiederkehr A, Avaro S, Prescianotto-Baschong C, Haguenauer-Tsapis R, Riezman H. The F-box protein Rcy1p is involved in endocytic membrane traffic and recycling out of an early endosome in *Saccharomyces cerevisiae*. J Cell Biol 2000;149:397–410.
29. Amerik AY, Li SJ, Hochstrasser M. Analysis of the deubiquitinating enzymes of the yeast *Saccharomyces cerevisiae*. Biol Chem 2000;381:981–992.
30. Hochstrasser M, Varshavsky A. *In vivo* degradation of a transcriptional regulator: the yeast α2 repressor. Cell 1990;61:697–708.
31. Swaminathan S, Amerik AY, Hochstrasser M. The Doa4 deubiquitinating enzyme is required for ubiquitin homeostasis in yeast. Mol Biol Cell 1999;10:2583–2594.
32. Amerik AY, Nowak J, Swaminathan S, Hochstrasser M. The Doa4 deubiquitinating enzyme is functionally linked to the vacuolar protein-sorting and endocytic pathways. Mol Biol Cell 2000;11:3365–3380.
33. Dupre S, Haguenauer-Tsapis R. Deubiquitination step in the endocytic pathway of yeast plasma membrane proteins: crucial role of Doa4p ubiquitin isopeptidase. Mol Cell Biol 2001;21:4482–4494.
34. Odorizzi G, Babst M, Emr SD. Fab1p PtdIns (3) P 5-kinase function essential for protein sorting in the multivesicular body. Cell 1998;95:847–858.
35. Stefan CJ, Blumer KJ. A syntaxin homolog encoded by *VAM3* mediates down-regulation of a yeast G protein-coupled receptor. J Biol Chem 1999;274:1835–1841.
36. Li Y, Kane T, Tipper C, Spatrick P, Jenness DD. Yeast mutants affecting possible quality control of plasma membrane proteins. Mol Cell Biol 1999;19:3588–3599.
37. Losko S, Kopp F, Kranz A, Kolling R. Uptake of the ATP-binding cassette (ABC) transporter Ste6 into the yeast vacuole is blocked in the *doa4* Mutant. Mol Biol Cell 2001;12:1047–1059.
38. Futter CE, Pearse A, Hewlett LJ, Hopkins CR. Multivesicular endosomes containing internalized EGF-EGF receptor complexes mature and then fuse directly with lysosomes. J Cell Biol 1996;132:1011–1023.
39. Panek HR, Stepp JD, Engle HM, Marks KM, Tan PK, Lemmon SK et al. Suppressors of *YCK*-encoded yeast casein kinase 1 deficiency define the four subunits of a novel clathrin AP-like complex. EMBO J 1997;16:4194–4204.
40. Dunn R, Hicke L. Multiple roles for Rsp5p-dependent ubiquitination at the internalization step of endocytosis. J Biol Chem 2001;276:25974–25981.
41. Mayor S, Presley JF, Maxfield FR. Sorting of membrane components from endosomes and subsequent recycling to the cell surface occurs by a bulk flow process. J Cell Biol 1993;121:1257–1269.
42. Gruenberg J, Maxfield FR. Membrane transport in the endocytic pathway. Curr Opin Cell Biol 1995;7:552–563.
43. Reggiori F, Black MW, Pelham HR. Polar transmembrane domains target proteins to the interior of the yeast vacuole. Mol Biol Cell 2000;11:3737–3749.
44. Katzmann DJ, Babst M, Emr SD. Ubiquitin-dependent sorting into the multivesicular body pathway requires the function of a conserved endosomal protein sorting complex, ESCRT-I. Cell 2001;106:145–155.
45. Urbanowski JL, Piper RC. Ubiquitin sorts proteins into the intralumenal degradative compartment of the late-endosome/vacuole. Traffic 2001;2:622–630.
46. Reggiori F, Pelham HR. Sorting of proteins into multivesicular bodies: ubiquitin-dependent and -independent targeting. EMBO J 2001;20:5176–5186.
47. Griffiths G, Hoflack B, Simons K, Mellman I, Kornfeld S. The mannose 6-phosphate receptor and the biogenesis of lysosomes. Cell 1988;52:329–341.
48. Raymond CK, Howald-Stevenson I, Vater CA, Stevens TH. Morpholog-

ical classification of the yeast vacuolar protein sorting mutants: evidence for a prevacuolar compartment in class E *vps* mutants. Mol Biol Cell 1992;3:1389–1402.

49. Piper RC, Cooper AA, Yang H, Stevens TH. *VPS27* controls vacuolar and endocytic traffic through a prevacuolar compartment in *Saccharomyces cerevisiae*. J Cell Biol 1995;131:603–617.
50. Levkowitz G, Waterman H, Zamir E, Kam Z, Oved S, Langdon WY, Beguinot L, Geiger B, Yarden Y. c-Cbl/Sli-1 regulates endocytic sorting and ubiquitination of the epidermal growth factor receptor. Genes Dev 1998;12:3663–3674.
51. Rocca A, Lamaze C, Subtil A, Dautry-Varsat A. Involvement of the ubiquitin/proteasome system in sorting of the interleukin 2 receptor beta chain to late endocytic compartments. Mol Biol Cell 2001;12:1293–1301.
52. Wach A, Brachat A, Pohlmann R, Philippsen P. New heterologous modules for classical or PCR-based gene disruptions in *Saccharomyces cerevisiae*. Yeast 1994;10:1793–1808.
53. Horton RM. In vitro recombination and mutagenesis of DNA. SOEing together tailor-made genes. Meth Mol Biol 1997;67:141–149.
54. Kunkel TA, Roberts JD, Zakour RA. Rapid and efficient site-specific mutagenesis without phenotypic selection. Meth Enzymol 1987; 154:367–382.
55. Kuchler K, Sterne RE, Thorner J. *Saccharomyces cerevisiae STE6* gene product: a novel pathway for protein export in eukaryotic cells. EMBO J 1989;8:3973–3984.
56. Siliciano PG, Tatchell K. Transcription and regulatory signals at the mating type locus in yeast. Cell 1984;37:969–978.